

Effect of Natural Fractures on Hydraulic Fracture Initiation in Cased Perforated Boreholes

Abstract. Hydraulic fracturing is a significant stimulation technology and method to enhance hydrocarbon recovery from low-permeability reservoirs. Accurate prediction of initiation pressure is a crucial step to make sure the success of hydraulic fracturing. Currently, predictive calculation of initiation pressure is for homogeneous formations; however, in fractured formations that has been a very complex issue all along. This paper assumes that natural fractures intersect with perforations, the tensile failure criteria is adopted and the calculation model of initiation pressure is presented for perforated wells of fractured formations considering that hydraulic fracture initiates from rock body of perforations surface or along natural fractures. The calculation results show that many factors have significant influence on the initiation pressure: the strike and dip of natural fractures, the intersecting position of natural fractures and perforations, the perforation orientation around borehole and the geostress orientation. The research results also suggest that not only the initiation pressure may sharply fall but also the initiation pressure difference for different orientation perforations may significantly become smaller due to the effect of natural fractures which will lead to hydraulic fractures' simultaneous initiation and propagation from different orientation perforations, so that complex near-wellbore multiple fractures develop. The comparative analysis of the actual and the calculation initiation pressure proves the accuracy and reliability of the calculation model. The established calculation model in this paper achieves the quantitative calculation of initiation pressure and simultaneously provides the theoretical basis to explain the physical phenomena of near-wellbore multiple fractures propagation for perforated wells of fractured formations.

Streszczenie. Metoda frakcjonowania hydraulicznego jest stosowana do odzyskiwania związków węglowodorowych a więc na przykład w technologii odzyskiwania gazu łupkowego. W artykule zaprezentowano model matematyczny tej technologii. (Efekt naturalnego frakcjonowania na przykładzie perforowanych otworów wiertniczych)

Keywords: Hydraulic fracture, Fractured formations, Initiation pressure, Natural fractures.

Słowa kluczowe: frakcjonowanie hydrauliczne, związki węglowodorowe

1. Introduction

Hydraulic fracturing has been widely used for a half century to improve oil and gas production from low-permeability reservoirs in the petroleum industry. For fractured reservoirs, complex near-wellbore fracture geometry is a common occurrence due to the effect of natural fractures [1]-[6]. This tortuous complex fracture geometry may lead to many problems, such as premature screen-out [7]-[8], low proppant concentrations [7], high treating pressure [9], and multiple fractures [10]-[12], etc. In general, one of these problems may have significant impact on other issues. However, the basic understanding of fracture initiation and extension can explain many of these problems in a way so that preventative measures can be devised during design of hydraulic fracturing treatments. In view of this, many researchers have tried to investigate these near-wellbore problems experimentally and theoretically, but they all only considered the effects of perforations and deviated wells and ignored the effect of natural fractures. This study makes theoretical efforts with a new thought to better understand the mechanism of fracture initiation in fractured formations.

Hydraulic fracturing initiation pressure has been extensively studied by many authors. Early initiation pressure equations are only for uncased vertical wells [13]-[15]. Later, deviated wells were drilled, the initiation pressure calculation model for deviated wells were established by considering the influence of well trajectory and the in situ stress distribution [16]-[18], and it was found that the initiated fracture tended to propagate in a curved path to reorient to a plane which was perpendicular to the minimum principle in situ stress. Some experimental studies proved the research results of the aforementioned calculation model [19]-[20]. Weng investigated the fracture initiation and propagation by applying a numerical model and found that the initiated fracture from the wellbore has a tortuous path in a distance close to the wellbore [21]. This result was found through experimental studies as well [22]. Some studies have been done for mitigating the near-wellbore fracture initiation problems [23]-[24]. When there is a risk of multiple fractures development, it is

suggested to use high concentration slugs of small size proppant to plug small fractures or low concentration slugs are suggested to erode the initial fracture and thus lessen the tortuosity.

After having a survey, it is found that, near-wellbore parameters are rather important to be considered in designing hydraulic fracturing. They affect greatly the fracture initiation and near-wellbore fracture geometry. Recent study always focuses on the effects of wellbore trajectory and perforation orientation, yet the influence of natural fractures has not been studied by any experiments and theories. Therefore, the paper will attempt to develop a new calculation model of initiation pressure for perforated wells of fractured formations.

2. Physical Model

Based on the spatial relationship of natural fracture plane and perforated tunnel, it is easy to get the diagram of natural fracture intersecting with perforated tunnel for the establishment of calculation model, referring to Fig.1.

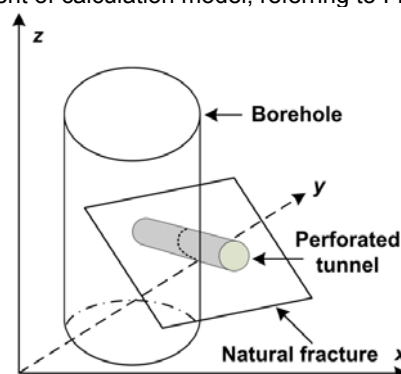


Fig.1. The intersection of natural fracture plane and perforated tunnel

3. Stress Profile over Perforation Surface

Generally there are three principle stresses in any underground formation, two of them are horizontal and the other one is vertical. Considering the rock around wellbore is

under the combined effects of far field stress and bottom hole fluid pressure, stresses in Cartesian coordinate systems can be converted into radial, tangential and axial stresses through the following equations [25]:

$$(1) \quad \sigma_r = \frac{r_w^2}{r^2} p_w + \frac{1}{2}(\sigma_H + \sigma_h) \left(1 - \frac{r_w^2}{r^2}\right) + \frac{1}{2}(\sigma_H - \sigma_h) \left(1 + \frac{3r_w^4}{r^4} - \frac{4r_w^2}{r^2}\right) \cos 2\theta$$

$$(2) \quad \sigma_\theta = -\frac{r_w^2}{r^2} p_w + \frac{1}{2}(\sigma_H + \sigma_h) \left(1 + \frac{r_w^2}{r^2}\right) - \frac{1}{2}(\sigma_H - \sigma_h) \left(1 + \frac{3r_w^4}{r^4}\right) \cos 2\theta$$

$$(3) \quad \sigma_z = \sigma_v - 2\nu(\sigma_H - \sigma_h) \left(\frac{r_w}{r}\right)^2 \cos 2\theta$$

$$(4) \quad \tau_{r\theta} = -\frac{1}{2}(\sigma_H - \sigma_h) \left(1 - \frac{3r_w^4}{r^4} + \frac{2r_w^2}{r^2}\right) \sin 2\theta$$

$$(5) \quad \tau_{z\theta} = \tau_{rz} = 0$$

where: σ_H =maximum horizontal stress, MPa; σ_h = minimum horizontal stress, MPa; σ_v =vertical stress, MPa; σ_r =wellbore radial stress, MPa; σ_θ =wellbore tangential stress, MPa; σ_z =wellbore axial stress, MPa; $\tau_{r\theta}$ =wellbore shear stress, MPa; p_w =wellbore pressure, MPa; r_w = wellbore radius, m; r =radial distance away from centre of wellbore, m; ν =Poisson's ratio, dimensionless; θ =the angle around wellbore circumference, deg.

Actually any fracture would be initiated along the perforated tunnel. So simulating the perforation stress profile is critically important. To do so, a perforation is assumed to be a micro-hole orthogonal to the well axis, and then the wellbore stress profile is applied to simulate the stress distribution of perforation.¹⁸ Perforations in space are subjected to the horizontal stress σ_θ , vertical stress σ_z , axial stress σ_r , and corresponding shear stress components. The same as the transformation of wellbore stresses, the transformation of stresses around perforation is shown in Fig.2.

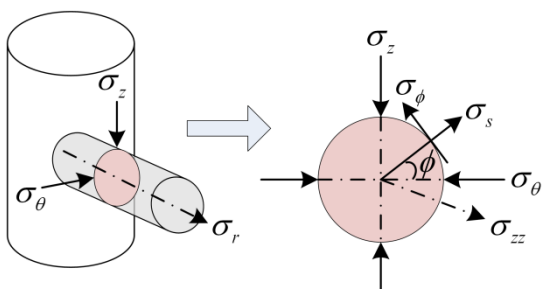


Fig.2. The stresses acting on perforated tunnel surface and the transformation of stresses

Taking into account the effect of fracturing fluid filtration on perforation rock stress, the radial, tangential and axial stresses over the surface of perforations are obtained through the following equations:

$$(6) \quad \sigma_s = p_w - \varphi(p_w - p_p)$$

$$(7) \quad \sigma_\phi = -p_w + (\sigma_\theta + \sigma_z) - 2(\sigma_\theta - \sigma_z) \cos 2\phi + \left[\frac{\alpha(1-2\nu)}{(1-\nu)} - \varphi \right] (p_w - p_p)$$

$$(8) \quad \sigma_{zz} = \sigma_r - 2\nu(\sigma_\theta - \sigma_z) \cos 2\phi + \left[\frac{\alpha(1-2\nu)}{(1-\nu)} - \varphi \right] (p_w - p_p)$$

$$(9) \quad \tau_{z\phi} = 2\tau_{r\theta} \sin \phi$$

$$(10) \quad \tau_{s\phi} = \tau_{sz} = 0$$

where: p_p =formation pore pressure, MPa; φ =formation porosity, dimensionless; α =biot's constant, dimensionless; ϕ =the angle around perforation circumference, deg.

Combining with composite stress theory [26], it is easy to obtain three principal stresses of any point over perforation surface:

$$(11) \quad \sigma_1 = \sigma_s$$

$$(12) \quad \sigma_2 = \frac{1}{2} \left[(\sigma_\phi + \sigma_{zz}) + \sqrt{(\sigma_\phi - \sigma_{zz})^2 + 4\tau_{z\phi}^2} \right]$$

$$(13) \quad \sigma_3 = \frac{1}{2} \left[(\sigma_\phi + \sigma_{zz}) - \sqrt{(\sigma_\phi - \sigma_{zz})^2 + 4\tau_{z\phi}^2} \right]$$

In fact, two mutually perpendicular stresses σ_ϕ and σ_{zz} rotate at a certain angle of γ in ϕ - z plane which is tangent to the perforation surface, then the principal stresses σ_2 and σ_3 can be obtained. The rotated angle γ just makes the shear stress equal to zero. The rotated angle can be calculated by the following equation:

$$(14) \quad \tan 2\gamma = \frac{2\tau_{z\phi}}{\sigma_\phi - \sigma_{zz}}$$

4. Calculation Model of Initiation Pressure

When the wellbore pressure is increased in the first step of a hydraulic fracturing operation, the fracturing fluid will initiate the fracture somewhere in the perforation tunnel, then hydraulic fracture can initiate from rock body of perforation surface or along natural fractures. Hence, the calculation model contains two different types of initiation modes, initiating from rock body of perforation surface and along natural fractures respectively.

4.1 Initiation from Rock Body

The maximum tensile stress of any point on perforation surface should be:

$$(15) \quad \sigma_{\max} = \sigma_3$$

Based on the tensile failure criteria, when the maximum effective tensile stress on perforation surface is less than rock tensile strength, the rock initiates:

$$(16) \quad \sigma_{\max} - \alpha p_p \leq -\sigma_t$$

Where: σ_t =rock tensile strength, MPa.

4.2 Initiation along Natural Fractures

When fluid pressure in natural fractures exceeds the effective normal stress acting on natural fracture plane, hydraulic fracture will initiate along natural fractures:

$$(17) \quad p_f \geq \sigma_n - \alpha p_p$$

where: p_f =fluid pressure in natural fractures, MPa; σ_n =normal stress acting on natural fracture plane, MPa.

From the principal stresses of the intersecting point of natural fractures and perforations, normal stress acting on natural fractures is:

$$(18) \quad \sigma_n = \cos^2 \beta_1 \sigma_1 + \cos^2 \beta_2 \sigma_2 + \cos^2 \beta_3 \sigma_3$$

where: σ_i =the principal stresses acting on natural fracture plane, MPa; β_i =the angle between the orientation of principal

stresses and the normal direction of natural fractures, deg.

According to spatial azimuth of natural fractures, we can get the normal direction vector of natural fractures in the earth coordinate systems:

$$(19) \quad \vec{n}_1 = a_1 i + a_2 j + a_3 k$$

where:

$$a_1 = -\sin(Dip)\cos(Ne)$$

$$a_2 = \sin(Dip)\sin(Ne) \quad a_3 = \cos(Dip)$$

where: Ne is the natural fractures strike, deg; Dip is the natural fractures dip, deg.

According to spatial azimuth of principal stresses over perforation surface, the direction vector of principal stress σ_1 in earth coordinate systems can be calculated:

$$(20) \quad \vec{n}_2(\sigma_1) = b_{1-1}i + b_{2-1}j + b_{3-1}k$$

where:

$$b_{1-1} = \cos(Ha + \theta)\cos(\phi)$$

$$b_{2-1} = \sin(Ha + \theta)\cos(\phi) \quad b_{3-1} = \sin(\phi)$$

where: Ha is the orientation of the maximum horizontal stress in the earth coordinate systems, deg; θ is angle between the perforation orientation and the orientation of the maximum horizontal stress, deg; ϕ is the circumferential angle around perforation from the orientation of the stress σ_θ , deg.

In a similar way, the direction vector of principal stress σ_2 in the earth coordinate systems is:

$$(21) \quad \vec{n}_2(\sigma_2) = b_{1-2}i + b_{2-2}j + b_{3-2}k$$

where:

$$b_{1-2} = \sin(Ha + \psi + \theta)\sqrt{\cos^2(\gamma) + \sin^2(\gamma)\sin^2(\phi)}$$

$$b_{2-2} = -\cos(Ha + \psi + \theta) \cdot$$

$$\sqrt{\cos^2(\gamma) + \sin^2(\gamma)\sin^2(\phi)}$$

$$b_{3-2} = -\cos(\phi)\sin(\gamma)$$

And ψ is:

$$\psi = \arctan \frac{\sin(\phi)\sin(\gamma)}{\cos(\gamma)}$$

Similarly, the direction vector of principal stress σ_3 in earth coordinate systems is:

$$(22) \quad \vec{n}_2(\sigma_3) = b_{1-3}i + b_{2-3}j + b_{3-3}k$$

where:

$$b_{1-3} = \sin(Ha + \omega + \theta)\sqrt{\sin^2(\gamma) + \cos^2(\gamma)\sin^2(\phi)}$$

$$b_{2-3} = -\cos(Ha + \omega + \theta) \cdot$$

$$\sqrt{\sin^2(\gamma) + \cos^2(\gamma)\sin^2(\phi)}$$

$$b_{3-3} = -\cos(\phi)\cos(\gamma)$$

And ω is:

$$\omega = \arctan \left[-\frac{\sin(\phi)\cos(\gamma)}{\sin(\gamma)} \right]$$

According to the normal direction vector of natural fractures and the direction vectors of principal stresses, the cosine of the angle between the direction of principal stresses and the normal direction of natural fractures can be expressed uniformly:

$$(23) \quad \cos \beta_i = \frac{\vec{n}_1 \cdot \vec{n}_2(\sigma_i)}{|\vec{n}_1| \cdot |\vec{n}_2(\sigma_i)|} \quad (i=1,2,3)$$

5. Results and Discussion

Based on the calculation model of initiation pressure, well B59-68 is exemplified for calculation. The well locates in Inner Mongolian Autonomous Region, China. The oil layer is volcanic rock, ranging from 1994.8-2013.0m in depth. Natural fractures distribute fully in the objective layer. The initiation pressure is calculated and analyzed by the data of well B59-68 listed in Table 1.

Table 1 Input data for the calculation of initiation pressure

Maximum horizontal stress[MPa]	47
Minimum horizontal stress[MPa]	39
Vertical stress[MPa]	50
Formation pore pressure[MPa]	24
Well radius[m]	0.1
Formation porosity	0.11
biot's constant	0.85
Poisson's ratio	0.22
Rock tensile strength[MPa]	7
Perforation depth[m]	0.5

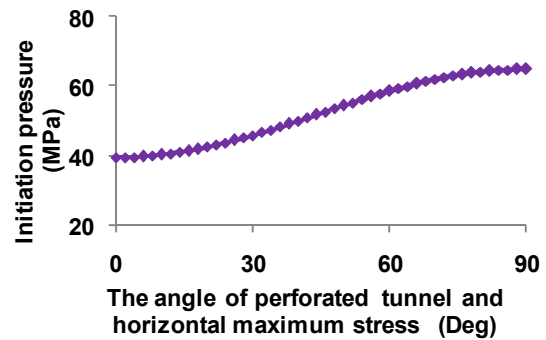


Fig. 3 The variation of rock body initiation pressure along with the orientation of perforated tunnel

5.1 Analysis of Initiation from Rock Body

Fig.3 shows the variation of rock body initiation pressure for different perforation orientations. From Fig.3 we can see the initiation pressure is the minimum value when the perforation orientation is parallel to the orientation of the maximum horizontal stress, it is 39.5MPa; the initiation pressure is the maximum value when the perforation orientation is parallel to the orientation of the minimum horizontal stress, it is 64.9MPa. Because the initiation pressure difference between the maximum and the minimum horizontal stress orientations is very large, hydraulic fracture will only initiate from the orientation of the maximum horizontal stress, which is the reason that simple, symmetrical, bi-wing and planar fracture produces during hydraulic fracturing in homogeneous formations.

5.2 Analysis of Initiation along Natural Fractures

In order to distinguish the hydraulic fracture initiation from rock body or along natural fractures, this paper makes following definitions: when the initiation pressure along natural fractures is not greater than that from rock body of perforations, hydraulic fracture will initiate along natural fractures.

Fig.4 shows that the initiation pressure along natural fractures changes with the depth of natural fractures intersecting with the perforated tunnel. With the increase of intersecting depth, the initiation pressure has the variation of first increase and then decrease. Because the initiation pressure from rock body equals 39.5MPa in this perforation orientation, hence, the initiation pressure along natural fractures is smaller than that from rock body of perforations.

Thus, it is clear that the initiation pressure of fractured formations can drastically reduce due to the effect of natural fractures.

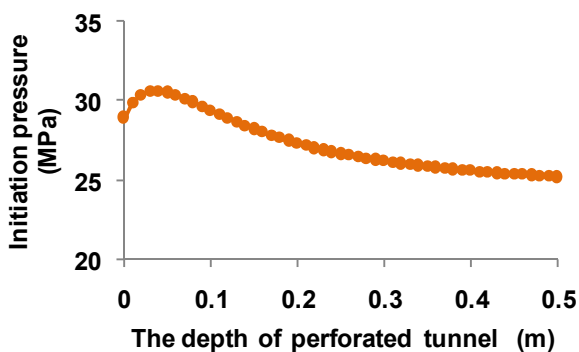


Fig. 4 The variation of initiation pressure along with the depth of perforated tunnel

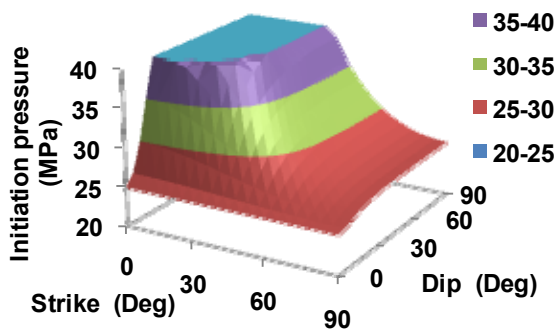


Fig. 5 The variation of initiation pressure along with strike and dip of natural fractures

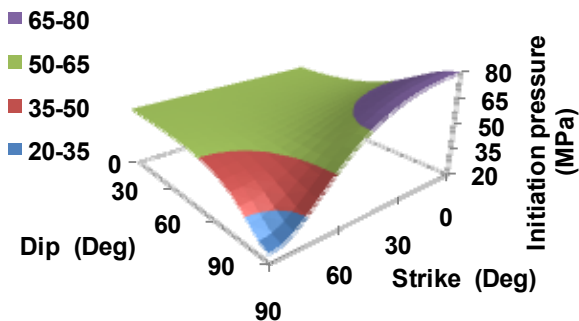


Fig. 6 The variation of initiation pressure along with strike and dip of natural fractures

Assuming that the orientation of the maximum horizontal stress is N90°E, perforation is in the orientation of the maximum horizontal stress, natural fractures and perforation intersect at the perforation top, effect of natural fractures' strike and dip on the initiation pressure along natural fractures is shown in Fig.5. Because the rock body initiation pressure is 39.5MPa in this perforation orientation, hydraulic fracture won't initiate along natural fractures in low strike and middle-high dip, but most likely initiates in the high strike or low dip.

The calculation parameters for Fig.5 remain unchanged, but natural fractures and perforation intersect at the horizontal position of perforation. The initiation pressure along natural fractures is shown in Fig.6. Compare Fig.5 with Fig.6, the smaller the circumferential angle around perforation is, the greater the initiation pressure will be and the more difficult hydraulic fracture initiating along natural

fractures will be.

The calculation parameters for Fig.5 remain unchanged, but assuming that perforation is in the orientation of the minimum horizontal stress, the initiation pressure along natural fractures is shown in Fig.7. Because the rock body initiation pressure is 64.9MPa in this perforation orientation, hence, at the intersecting point, hydraulic fracture will initiate along natural fractures in any combination of strike and dip. Compare Fig.5 with Fig.7, when the perforation orientation is under the two extreme orientations of the maximum and minimum horizontal stress, the initiation pressure along natural fractures are both in the range of 25-30MPa at low dip, hence, the initiation pressure difference of the two extreme perforation orientations may significantly become smaller due to the effect of natural fractures which may lead to hydraulic fractures' simultaneous initiation and propagation from different orientation perforations around wellbore so that multiple fractures will extend.

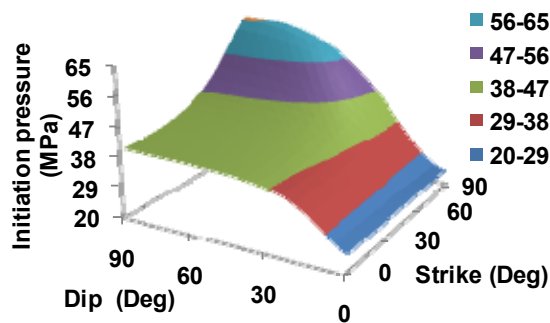


Fig. 7 The variation of initiation pressure along with strike and dip of natural fractures

The calculation parameters for Fig.7 remain unchanged, but the orientation of the maximum horizontal stress is changed to N45°E, the initiation pressure along natural fractures is shown in Fig.8. Compare Fig.7 with Fig.8, the geostress orientation in the earth coordinate systems seriously influences the initiation pressure. On the whole, initiation pressure becomes smaller, from the maximum range 60-65MPa in Fig.7 to 40-45MPa in Fig.8, which means that hydraulic fracture is easier to initiate from different orientations. Hence, this effect will aggravate hydraulic fractures' initiation and extension from different orientation perforations.

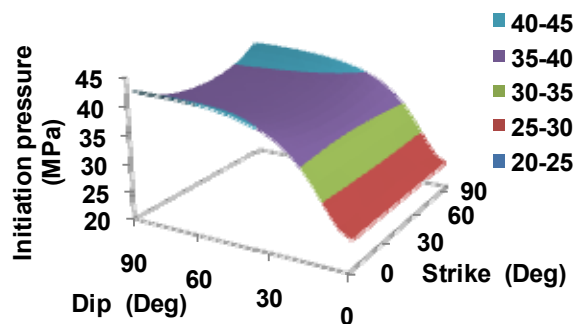


Fig. 8 The variation of initiation pressure along with strike and dip of natural fractures

5.3 Analysis for Model Validation

For well B59-68, the orientation of the maximum horizontal stress in the objective layer is N72°E by using wellbore caving method; according to core description and imaging logs, the natural fractures' strike is 45° and the natural fractures' dip is N20°E. It is calculated that the initiation pressure is 30.56MPa and 30.1MPa when perforation is in the maximum and minimum horizontal

stress orientations respectively. The initiation pressure difference is only 0.46MPa in the two extreme perforation orientations. Therefore, hydraulic fractures will initiate and propagate easily from different orientation perforations around wellbore.

On August 4, 2010, test fracturing was carried out in this well. The actual initiation pressure was 29.2MPa, and the relative error of calculation value was 3.1%, which is within the range of engineering permissible error. This confirmed the accuracy of this calculation model. According to the micro-seismic monitoring results of fractures' extension during main fracturing, the primary fissures near the wellbore were fully developed, and the extension orientations were N58°-75°E, N15°W and N28°W respectively. Hence, the propagation of fractures has the characteristics of multi-fractures extension. It also confirmed the theoretical inference of multiple fractures extension for well B59-68.

6. Conclusion

Based on a new idea, the impact of natural fractures in cased perforated boreholes on hydraulic fracture initiation is studied in this paper. This calculation model in the paper achieves the quantitative calculation of initiation pressure for perforated wells in fractured formations. The initiation pressure may drastically reduce and the initiation pressure difference for different orientation perforations around wellbore may significantly become smaller due to the effect of natural fractures. Hence, the calculation model can also explain the propagation mechanism of multiple fractures and provides a theoretical basis to optimize the design of hydraulic fracturing for fractured formations.

Acknowledgments

The work was supported by special fund of China's central government for the development of local colleges and universities — the project of national first-level discipline in Oil and Gas Engineering.

REFERENCES

- [1] Maxwell S.C., Urbancic T.I., Steinsberger N., Zinno R., Microseismic imaging of hydraulic fracture complexity in the Barnett shale, SPE Annual Technical Conference and Exhibition, (2002) September 29- October 2, San Antonio, Texas
- [2] Urbancic T.I., Maxwell S.C., Microseismic imaging of fracture behavior in naturally fractured reservoirs, SPE/ISRM Rock Mechanics Conference, (2002) October 20-23, Irving, Texas
- [3] Fisher M.K., Wright C.A., Davidson B.M., Goodwin A.K., Fielder E.O., Buckler W.S., Steinsberger N.P., Integrating fracture mapping technologies to optimize stimulations in the Barnett shale, SPE Annual Technical Conference and Exhibition, (2002) September 29- October 2, San Antonio, Texas
- [4] Fisher M.K., Heinze J.R., Harris C.D., Davidson B.M., Wright C.A., Dunn K.P., Optimizing horizontal completion techniques in the Barnett shale using microseismic fracture mapping, SPE Annual Technical Conference and Exhibition, (2004) September 26-29, Houston, Texas
- [5] Warpinski N.R., Teufel L.W., Influence of geologic discontinuities on hydraulic fracture propagation, JPT, 39, 209 (1987)
- [6] Warpinski N.R., Hydraulic fracturing in tight, fissured media, JPT, 43, 146 (1991)
- [7] Cleary M.P., Johnson D.E., Kogsbøll H-H., Owens K.A., Perry K.F., de Pater C.J., Alfred Stachel., Holger Schmidt., Mauro Tambini., Field Implementation of proppant slugs to avoid premature screen-out of hydraulic fractures with adequate proppant concentration, Low Permeability Reservoirs Symposium, (1993) April 26- 28, Denver, Colorado
- [8] Aud W.W., Wright T.B., Cipolla C.L., Harkrider J.D., The effect of viscosity on near-wellbore tortuosity and premature screenouts, SPE Annual Technical Conference and Exhibition, (1994) September 25-28, New Orleans, Louisiana
- [9] Davidson B.M., Saunders B.F., Robinson B.M., Holditch S.A., Analysis of abnormally high fracture treating pressures caused by complex fracture growth, SPE Gas Technology Symposium, (1993) June 28-30, Calgary, Alberta, Canada
- [10] Jeffrey R.G., Vandamme L., Roegiers J.C., Mechanical interactions in branched or subparallel hydraulic fractures, SPE/DOE Low Permeability Reservoirs Symposium, (1987) May 18-19, Denver, Colorado
- [11] Narendran V.M., Analysis of growth and interaction of multiple hydraulic fractures, SPE Reservoir Simulation Symposium, (1983) November 15-18, San Francisco, California
- [12] Lehman L.V., Brumley J.L., Etiology of multiple fractures, SPE Production Operations Symposium, (1997) March 9-11, Oklahoma City, Oklahoma
- [13] Howard G.C., Fast C.R., Theory of hydraulic fracturing, SPE of AIME, New York (1970)
- [14] Haimson B., Fairhurst C., Initiation and extension of hydraulic fractures in rocks, SPEJ, 7, 310 (1967)
- [15] Haimson B., Fairhurst C., Hydraulic fracturing in porous-permeable materials, JPT, 21, 811 (1969)
- [16] Yew C.H., Li Y., Fracturing of a deviated well, SPE Production Engineering, 429, 3 (1988)
- [17] Olson J.E., Fracturing from highly deviated and horizontal wells: numerical analysis of non-planar fracture propagation, Low Permeability Reservoirs Symposium, (1995) March 19-22, Denver, Colorado
- [18] Fallahzadeh S.H., Shadizadeh S.R., Pourafshary P., Dealing with the challenges of hydraulic fracture initiation in deviated -cased perforated boreholes, Trinidad and Tobago Energy Resources Conference, (2010) June 27-30, Port of Spain, Trinidad
- [19] Berhmann L.A., Elbel J.L., Effect of perforations on fracture initiation, JPT, 43, 608 (1991)
- [20] van de Ketterij R.G., de Pater C.J., Experimental study on the impact of perforations on hydraulic fracture, SPE European Formation Damage Conference, (1997) June 2-3, The Hague, Netherlands
- [21] Weng X.W., Fracture initiation and propagation from deviated wellbores, SPE Annual Technical Conference and Exhibition, (1993) October 3-6, Houston, Texas
- [22] Abass H.H., Brumley J.L., Venditto J.J., Oriented perforations - a rock mechanics view, SPE Annual Technical Conference and Exhibition, (1994) September 25-28, New Orleans, Louisiana
- [23] Gulrajani S.N., Romero J., Evaluation and modification of fracture treatments showing near-wellbore effects, European Petroleum Conference, (1996) October 22-24, Milan, Italy
- [24] McDaniel B.W., McMechan D.E., Stegent N.A., Proper use of proppant slugs and viscous gel slugs can improve proppant placement during hydraulic fracturing applications. SPE Annual Technical Conference and Exhibition, (2001) September 30-October 3, New Orleans, Louisiana
- [25] Fjaer E., Holt R.M., Raaen A.M., Risnes R., Petroleum related rock mechanics, Elsevier Publications, London (2008)
- [26] Jaeger C.J., Cook N.G.W., Zimmerman R.W., Fundamentals of rock mechanics, Blackwell Publishing, Oxford (2007)

Authors: L. Ren, J. Z.Zhao, Y. Q.Hu and L. Wang are with the State Key Laboratory of Oil-Gas Reservoir Geology & Exploitation, Southwest Petroleum University, Chengdu, Sichuan, China.
(E-mail: renlanswpu@163.com.cn; zhaojz@swpu.edu.cn; stimswpi@163.com.cn; sweet_leilei@126.com.cn)